

## Optimal distribution of viscous dissipation in a multi-scale branched fluid distributor

L. Luo<sup>a,\*</sup>, D. Tondeur<sup>b</sup>

<sup>a</sup> *LOCIE, ESIGEC Université de Savoie, Chambéry, France*

<sup>b</sup> *Laboratoire des Sciences du Génie Chimique du CNRS, ENSIC-INPL, Nancy, France*

Received 25 April 2005; accepted 31 August 2005

Available online 27 October 2005

### Abstract

This paper examines some theoretical aspects of the optimal design of multi-scale fluid distributors or collectors, built on a binary or quaternary branching pattern of pores. The design aims to distribute uniformly a fluid flow over a specified square surface (uniform irrigation) while simultaneously minimizing the residence time, the residence-time distribution, the pressure drop and the viscous dissipation, leading to an optimization problem of the pore-size distribution, for both length and diameter. For the binary branching, the uniform distribution of outlet points requires a particular, non-monotonous scaling law for pore lengths, and this distinguishes the structure from fractal branching patterns that have been studied previously. The quaternary branching allows a fractal-type structure (constant scale ratios for both pore length and radius). An important general result is established: in the optimal pore-size distribution, *the density of viscous dissipation power ( $\text{W}\cdot\text{m}^{-3}$ ) is uniformly distributed over the volume at all scales.*

© 2005 Elsevier SAS. All rights reserved.

*Keywords:* Multi-scale optimization; Fluidics; Constructal

### 1. Introduction

The present article is concerned with the design of fluid distributors or collectors for multi-tubular or multi-pore devices such as cross-flow heat exchangers, monolithic catalysts, adsorption columns or the like. For this purpose, we consider branching networks such as that illustrated on Fig. 1. Properties expected from a “good” distributor are equidistribution of the flow-rate (uniform irrigation), minimal dispersion, minimal void volume, minimal pressure drop, leading necessarily to some compromise. The reason for minimizing void volume is best understood when one considers operations like start-up, rinsing, back-washing, displacement, elution, change of solvent or depressurization. For a given flow-rate, minimizing void volume obviously also implies minimizing the mean residence-time, and equidistribution of the flow is essential to minimizing the residence time distribution.

This problem may be approached using the so-called “*constructal theory*”, developed by Bejan and his co-workers from 1996 on, a quite general theory of multi-scale shapes and structures in nature and engineering [1–3]. The specific approach presented here starts from [4] and extends this work with some new results and new situations.

In “constructal” terms, the distributor or collector problem is topologically one of connection between a point and a surface. The “point” is here the single inlet tube or pore, and the surface is the domain that must be fed by the distributed flow. The approach will be restricted here to square or rectangular outlet surfaces. Let us first describe the distributor/collector of Fig. 1.

### 2. A branched fluid distributor

#### 2.1. Description

The solid pyramidal block of Fig. 1 has an internal pore network shown in Fig. 2; its projection on the “base plane”

\* Corresponding author.

*E-mail address:* [lingai.luo@univ-savoie.fr](mailto:lingai.luo@univ-savoie.fr) (L. Luo).

**Nomenclature**

$a$	parameter in pressure-drop relation (Eq. (8)) (dimension depends on flow model)	$N$	number of outlet ports of distributor
$A$	$= (a\mu)/2\pi^2$ , defined by Eq. (12) (dimension depends on flow model)	$p, q$	parameters in pressure-drop relation (Eq. (14))
$d_k$	viscous dissipation power in single pore of class $k$ .....	$r_k$	radius of pore of class $k$ .....
	$J \cdot s^{-1}$	$u_k$	fluid velocity in pore of class $k$ .....
	$m \cdot s^{-1}$	$v_k$	volume of a single pore of class $k$ .....
$D_k$	total viscous dissipation power in pores of class $k$ .....	$V_k$	total volume of pores of class $k$ .....
	$J \cdot s^{-1}$	$V_p$	total pore volume of the structure .....
$D_{tot}$	total viscous dissipation power in structure .....	$\Delta p_k$	pressure drop in pore of class $k$ .....
	$J \cdot s^{-1}$	$\varepsilon$	volume fraction, porosity
$f_k$	flow-rate in single pore of class $k$ .....	$\Phi$	Lagrangian function (Eq. (10))
	$m^3 \cdot s^{-1}$	$\lambda$	Lagrange multiplier
$f_0$	total flow-rate in structure .....	$\mu$	fluid viscosity .....
	$m^3 \cdot s^{-1}$	$\Psi$	general distribution function of pore volume and dissipation
$l_k$	length of pore of class $k$ .....		
	$m$		
$L$	width of outlet face of structure .....		
	$m^2$		
$m$	total number of scales (maximum value of $k$ )		
$n_k$	number of pores of class $k$		

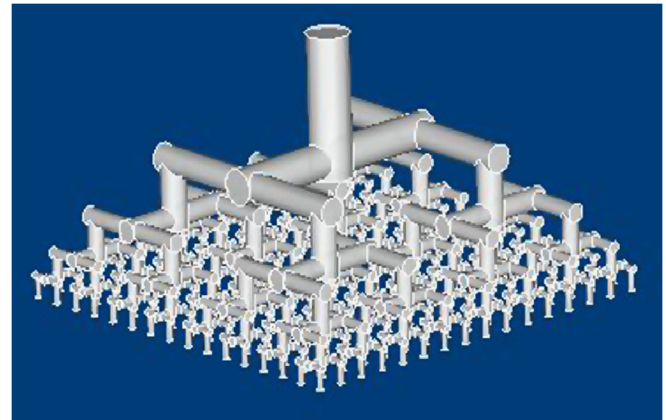
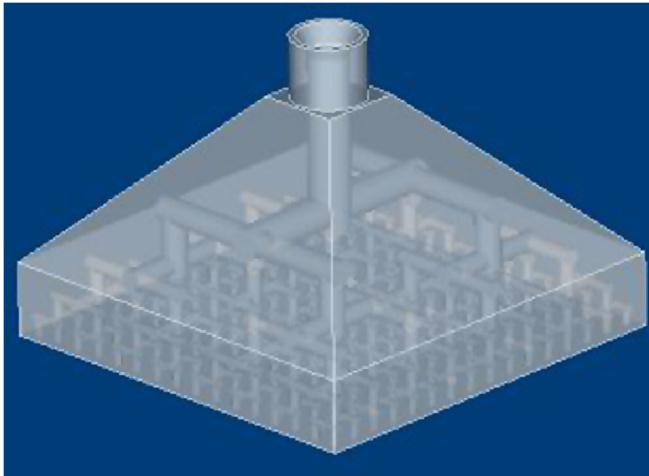


Fig. 2. Pore structure of binary-branched fluid distributor.

Fig. 1. Prototype of binary-branched fluid distributor for uniform irrigation; dimensions of base: 6 × 6 cm; smallest pore radius at outlet: 0.75 mm.

representing the irrigated surface is shown in Fig. 3. It has the structure of a sequence of 8 generations of *T*- or *Y*-bifurcations or divisions. The resulting pores are indexed from 0 to 8, including the inlet pore (index 0). The latter is split perpendicularly into two opposing pores (index 1), and each of these is again split into two pores (index 2), such that pores of index 1 and 2 are coplanar. These three successive generations of pores form the basic pattern, the elementary cell, which will be reproduced at smaller scales. Since there are 8 generations of bifurcations, there are  $2^8 = 256$  final outlet pores, open on the outlet face of this “pyramid”. It is of course in principle possible to continue the dichotomy to generate say  $2^9$  or  $2^{10}$  outlet ports. The present distributor was designed to distribute equally an input flow on a square surface with a “resolution” of approximately 8 outlet ports per  $cm^2$ , corresponding to a theoretical outlet surface of  $32 cm^2$  (side = 5.66 cm) and was manufactured by laser polymerization stereolithography [5].

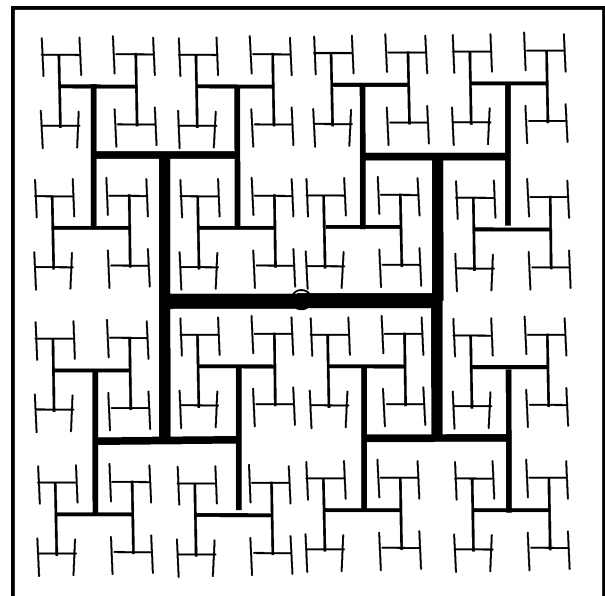


Fig. 3. Projection of pore network on base plane.

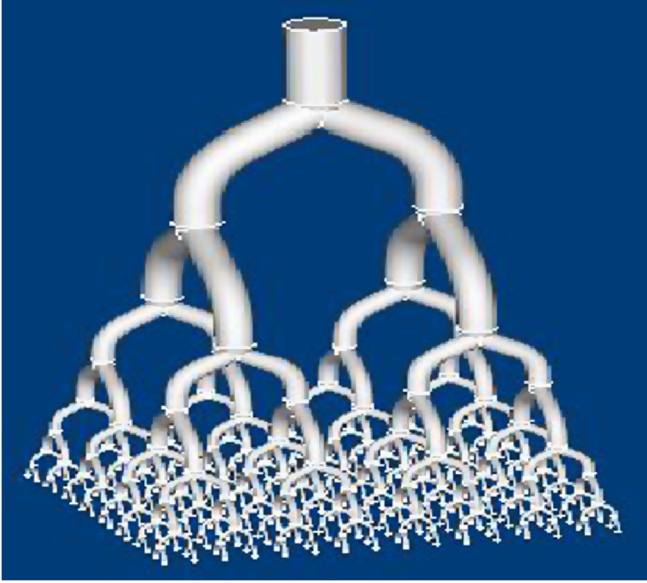


Fig. 4. Pore network with smooth direction changes.

Different variants of this structure may be produced. Figs. 1 and 2 illustrate a design where the changes in flow direction are sharp, but it may be designed with smooth changes as in Fig. 4, implying smaller pressure drop, but larger pore volume and overall volume (less compactness). The most compact design is a “flat” distributor in which all channels are embedded in the same “layer”. This is possible only if the largest channel is narrower than the distance separating two outlet ports [4].

## 2.2. Number of bifurcations and scaling laws for horizontal pore lengths

Let  $L$  be the length of the side of the square outlet face. Then the two branches or pores of generation 1 have a horizontal length  $l_1 = L/4$ , and the pores of the second generation have the same length  $l_2 = L/4$ . The four end points of these pores are located in the centre of the four squares subdividing the outlet face. This uniform distribution property should be conserved in subsequent constructions. The third generation of pores have a length  $l_3 = L/8$ , and their 8 end points cannot be uniformly distributed since it is not possible to subdivide a square into 8 equal squares. Only at generation 4 will this be possible again, with  $l_4 = L/8$ . Generally speaking, to achieve uniform distribution of end points, thus of potential outlet ports, two conditions are required:

- an even number of generations  $m$ ; this produces a number of end points that is an even power of 2 and the square of an integer, such as  $4 = 2^2$ ,  $16 = 2^4$ ,  $64 = 2^6$ ,  $256 = 2^8$ , etc.
- conservation of horizontal pore length when going from an odd to an even generation, and dividing by 2 the pore length when going from even to odd.

The result of this accounting, evidenced on Fig. 3, is summarized as follows:

Number of pores for any generation of index  $k$ :

$$n_k = 2^k \quad (1)$$

Number of end points (outlet ports) for  $m$  generations:

$$N = 2^m \quad (2)$$

Total number of pores:

$$n_t = \sum n_k = 2(2^m - 1) \quad (3)$$

Scaling laws for pore lengths:

$$l_k = \frac{L}{2^{(k+2)/2}} \quad \text{if } k \text{ even}$$

$$l_k = \frac{L}{2^{(k+3)/2}} \quad \text{if } k \text{ odd}$$

$$\frac{l_k}{l_{k+2}} = 2 \quad (4)$$

Total “horizontal” path length from inlet to outlet, with  $m$  even:

$$l_{\text{tot}} = \sum_{k=1}^{k=m} l_k = L[1 - 2^{-m/2}] \quad (5)$$

This length clearly converges towards  $L$  when  $m$  increases, in other words, the path length of the fluid is smaller than  $L$  but close to it (about  $0.94 L$  for  $m = 8$ ).

This construct is therefore such that *the 256 flow paths* from the unique inlet to any one of the 256 outlets *are strictly identical*. The flow-rate through all outlet ports and the residence times in the 256 paths should be identical, satisfying by construction the equidistribution property, but also minimal dispersion of residence time. In the approach developed above, the pore lengths are entirely determined by the overall size of the distributor and the constraint of uniform outlet distribution. No other consideration is introduced, and in particular, *the length distribution is fully independent of the pore radii*, to be determined below. The object developed here is not a fractal in the usual sense, because the pore length distribution (Eq. (4)) cannot be described by a fractal dimension. The object is not “scale-invariant” but rather “scale-covariant” [3]. Let us now consider the question of pore diameters.

## 3. Optimization of the pore size distribution

### 3.1. Constitutive equations

The distribution of pore radii  $r_k$  will be determined by an optimization that specifies the total flow-rate  $f_0$  and accounts for both *viscous dissipation and total pore volume*  $V_p$ . One of these constraints alone will not yield an optimal size distribution: minimizing the volume would lead to infinitely thin pores, and minimizing pressure drop or dissipation would result in as large pores as possible. The constitutive relations of our model for a single pore of length  $l_k$  and radius  $r_k$  are summarized below and comprise relations for the flow-rate  $f_k$  ( $\text{m}^3 \cdot \text{s}^{-1}$ ), the pore volume  $v_k$  ( $\text{m}^3$ ), the pressure drop  $\Delta p_k$  (Pa), and the dissipation  $d_k$  (W)

$$f_k = f_0/2^k \tag{6}$$

$$v_k = \pi l_k r_k^2 \tag{7}$$

$$\Delta p_k = \frac{a\mu}{\pi} \frac{f_k^q l_k}{r_k^p} \tag{8}$$

$$d_k = f_k \Delta p_k \tag{9}$$

where  $a$  is a numerical constant.

The form of the pressure drop expression (Eq. (8)) is analogous to Poiseuille’s law (for which  $q = 1$ ,  $p = 4$ ,  $a = 8$ ). The parameters  $a$ ,  $p$  and  $q$  account for the departure from established laminar flow and for the presence of flow singularities (bifurcations and changes in direction). Assuming isothermal incompressible flow, entropy production is proportional to dissipation. Note that if bifurcations are replaced by “multi-furcations”, where a pore is subdivided into  $w$  sub-pores, Eqs. (1) and (6) may be generalized, the factor 2 being replaced by  $w$ , but the length determination of the previous section must be revisited entirely.

### 3.2. Lagrangian optimization for minimal total dissipation

The optimization problem considered is to find the pore size distribution that *minimizes the total dissipation  $D_{tot}$  subject to the constraint of constant total pore volume  $V_p$* . For this purpose, we introduce the Lagrangian function  $\Phi$ , a linear combination of the two quantities defined above, dissipation and pore volume, expressed as sums over all channels of the expressions in Eqs. (9) and (7), respectively:

$$\begin{aligned} \Phi &= \sum_{k=1}^m 2^k f_k \Delta p + \lambda \left( \sum_{k=1}^m 2^k \pi l_k r_k^2 - V_p \right) \\ &= \sum_{k=1}^m 2^k \left[ \frac{a\mu}{\pi} \frac{f_k^{q+1} l_k}{r_k^p} + \lambda \pi l_k r_k^2 \right] - \lambda V_p \end{aligned} \tag{10}$$

where  $\lambda$  is a Lagrange multiplier. We shall refer to the two terms in the bracket of the right-hand side as the *dissipation term*, and the *hold-up term*, respectively. At specified overall flow-rate  $f_0$  and pore lengths  $l_k$ , this relation is differentiated with respect to  $\lambda$  and to each  $r_k$ , and the derivatives are cancelled (Euler equations) to find the conditions of an extremum of  $\Phi$ . It is possible to verify that this extremum is a minimum (the second derivatives of  $\Phi$  with respect to  $r_k$  are positive). These calculations are straightforward and only some end results are given below:

Ratio of dissipation to pore volume

$$\frac{d_k}{v_k} = \frac{D_k}{V_k} = \frac{D_{tot}}{V_p} = \frac{2\lambda}{p} \quad (k = 1, \dots, m) \tag{11}$$

Optimal pore radius

$$\begin{aligned} r_k^{p+2} &= \frac{pA}{\lambda} f_k^{q+1} = \frac{pA}{\lambda} f_0^{q+1} 2^{-(q+1)k} \\ \text{with } A &= \frac{a\mu}{2\pi^2} \quad (k = 1, \dots, m) \end{aligned} \tag{12}$$

Relation for Lagrange multiplier

$$\begin{aligned} \left[ \frac{pA}{\lambda} \right]^{-2/(p+2)} &= \frac{\pi}{V_p} \sum_k 2^k l_k f_k^b \\ \text{with } b &= 2 \frac{q+1}{p+2} \quad (k = 1, \dots, m) \end{aligned} \tag{13}$$

Let us examine the meaning of these relations. Eq. (11) expresses that the two contributions to the Lagrangian function, volume and dissipation, are in the same constant ratio in all channels, at all scales, including that of the whole construct. This is a form of “equipartition of irreversibilities” [7], where the space variable over which equipartition occurs is the pore volume. We shall express this fundamental result in a formal fashion as the following theorem, where the dissipation density is defined as dissipation per unit volume ( $W \cdot m^{-3}$ ):

#### Theorem of uniform dissipation density

*The pore size distribution that minimizes viscous dissipation (or entropy production), at constrained pore volume, is such that dissipation density is uniform in the whole construct.*

Note that dissipation density ( $W \cdot m^{-3}$ ) is closely related but not equivalent to pressure drop ( $J \cdot m^{-3}$ ). We discuss this point further in the conclusion section.

Eq. (12) tells that the optimal radius depends on the scale  $k$  only through a numerical factor (the parameters contained in  $A$ ,  $\lambda$  and  $f_0$  are independent of  $k$ ). In addition, this relation is *independent of pore length*. Recall that the pore length is determined by the outlet surface (actually, by the length  $L$ ) and the equidistribution constraint. We shall see further below the consequences of these properties on the relations between scales. To obtain an explicit relation for the optimal radius, we first need to exploit Eq. (13).

Note that all quantities involved in Eq. (13), including the summation, are calculable constants, characteristic of the construct as a whole, and of the total flow-rate  $f_0$  but independent of the particular scale index  $k$ . In other words, the Lagrange multiplier  $\lambda$  is a property of the construct as a whole. To make this more explicit, let us eliminate the  $f_k$  using Eq. (6), and the  $l_k$  by introducing the ratios  $l_k/L$  obtained from Eq. (4). Eq. (13) may then be recast in the following form:

$$\begin{aligned} \left( \frac{pA}{\lambda} \right)^{-2/(p+2)} \frac{V_p}{\pi L f_0^b} &= \sum_{k=1}^m 2^{k(1-b)} \frac{l_k}{L} \\ &= \left[ \sum_{k \text{ even}}^m 2^{k(1-b)} \cdot 2^{-(k+2)/2} + \sum_{k \text{ odd}}^{m-1} 2^{k(1-b)} \cdot 2^{-(k+3)/2} \right] \\ &= \sigma(m) \end{aligned} \tag{14}$$

The way the upper limit of the summations in the bracket are written assumes that  $m$  is even, as discussed in Section 2.2. Recall that for Poiseuille flow, the parameter  $b$  is equal to  $2/3$ . It can be seen that the bracket is independent of the physical quantities (flow-rate, viscosity, size  $L$  of the construct, pore size distribution), and depends only on the number of scales  $m$  and on the hydrodynamic law through  $b$ . It is therefore a sort of “universal” function, characteristic of the binary tree topology described here. We designate this function by  $\sigma(m)$  and call

it a “constructal function”. Indeed, we shall see that the properties of the optimal construct may be expressed in terms of  $\sigma(m)$ , and similar non-dimensional functions are generated by other constructal optimizations. Owing to its general interest, we give some more attention to its peculiar properties.

### 3.3. Properties of the constructal function $\sigma(m)$

Observe first that  $\sigma(m)$  is composed of two series, one with  $k$  even, the other with  $k$  odd. Let us illustrate these series for Poiseuille flow, i.e.  $b = 2/3$ . The exponents of the generic terms are then  $-(k + 6)/6$  for  $k$  even, and  $-(k + 9)/6$  for  $k$  odd. The explicit form of the two series and their summation are as follows:

$$\begin{aligned} \sigma_{\text{even}} &= \frac{1}{2^{4/3}} + \frac{1}{2^{5/3}} + \frac{1}{2^{6/3}} + \frac{1}{2^{7/3}} + \dots + \frac{1}{2^{(m+6)/6}} \\ &= \frac{2^{-4/3} - 2^{-(m+6)/6} \cdot 2^{-1/3}}{1 - 2^{-1/3}} = 1.924(1 - 2^{-m/6}) \\ \sigma_{\text{odd}} &= \frac{1}{2^{5/3}} + \frac{1}{2^{6/3}} + \frac{1}{2^{7/3}} + \frac{1}{2^{8/3}} + \dots + \frac{1}{2^{(m+8)/6}} \\ &= \frac{2^{-5/3} - 2^{-(m+8)/6} \cdot 2^{-1/3}}{1 - 2^{-1/3}} = 1.527(1 - 2^{-m/6}) \end{aligned} \quad (15)$$

These are geometric series with the same factor  $2^{-1/3}$  and differing only by the first and last terms. Their summation is therefore straightforward and given in Eq. (15). The final compact form of  $\sigma(m)$  for Poiseuille flow and  $m$  even is thus:

$$\sigma(m) = 3.451[1 - 2^{-m/6}] \quad (16)$$

Fig. 5 illustrates this function graphically.

The optimal properties may be expressed in terms of this quantity. Let us substitute the expression for  $A/\lambda$  obtained from Eq. (14) into the expression for the optimal radius, Eq. (12). We find that the flow-rate  $f_0$  cancels out and the final expression for  $r_{k,\text{opt}}$  is conveniently written as:

$$r_k^2 = \frac{2^{-bk} V_p}{\pi L \sigma(m)} \quad (17)$$

This expression may be substituted into the expressions for total pressure drop or total dissipation for example. Some manipulations are required to transform the summations into the

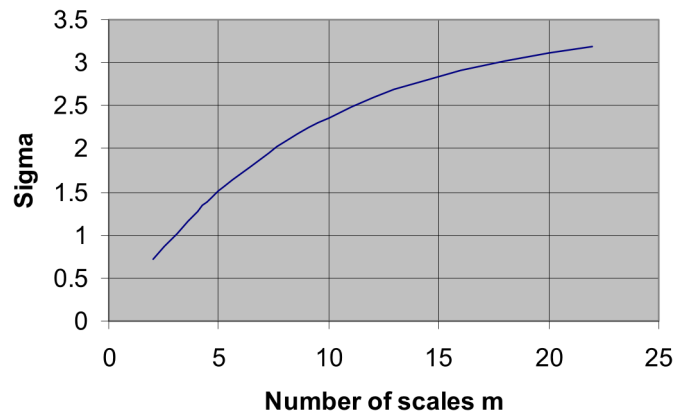


Fig. 5. The constructal function  $\sigma$  for the binary branching structure.

constructal function  $\sigma$ . Eq. (18) illustrates intermediate calculations for pressure drop, using successively Eqs. (8), (17), (13) for the definition of  $b$ , and (14) for the definition of  $\sigma$ :

$$\begin{aligned} \Delta P_{\text{tot}} &= \sum_{k=1}^m \Delta p_k = \frac{a\mu L f_0^q}{\pi} \sum_{k=1}^m \frac{l_k}{L} \frac{2^{-qk}}{r_{k,\text{opt}}^p} \\ &= \frac{a\mu L f_0^q}{\pi} \left[ \frac{\pi L \sigma}{V_p} \right]^{p/2} \sum_{k=1}^m \frac{l_k}{L} \frac{2^{-qk}}{2^{-bpk/2}} \\ &= 2A f_0^q (\pi L \sigma)^{p/2+1} V_p^{-p/2} \end{aligned} \quad (18)$$

The last equality results from the fact that the last summation is equal to  $\sigma$ . For Poiseuille flow, Eq. (18) reduces to:

$$\Delta P_{\text{tot}}(\text{Poiseuille}) = 8\pi \mu f_0 \frac{(L\sigma)^3}{V_p^2} \quad (19)$$

Total dissipation is simply obtained from total pressure drop by multiplying by the total flow-rate, as may be verified in Eq. (20):

$$\begin{aligned} D_{\text{tot}} &= \sum_{k=1}^m 2^k f_k \Delta p_k = \sum_{k=1}^m 2^k \frac{f_0}{2^k} \Delta p_k \\ &= f_0 \sum \Delta p_k = f_0 \Delta P_{\text{tot}} \end{aligned} \quad (20)$$

Dissipation has therefore the same power dependence as pressure drop on all variables except flow-rate.

## 4. Scaling laws and distributions

### 4.1. Scaling law for pore radii

Scaling laws are relations between quantities pertaining to different scales or generations. Eqs. (12) or (17) is used to generate a relation between pore radii of different generations. For this purpose, consider a bifurcation of a pore of radius  $r_k$  with flow-rate  $f_k$ , into two pores of radii  $r_{k+1}$  with flow-rate  $f_k/2$ . Writing for example Eq. (12) twice, for  $r_k$  and  $r_{k+1}$ , and dividing the two expressions, one gets:

$$\begin{aligned} \left( \frac{r_k}{r_{k+1}} \right)^{p+2} &= \left( \frac{f_k}{f_{k+1}} \right)^{q+1} = 2^{q+1} = \left( \frac{u_k}{u_{k+1}} \right)^{p+2} \quad \text{or} \\ \frac{r_k}{r_{k+1}} &= \frac{u_k}{u_{k+1}} = 2^{b/2} \end{aligned} \quad (21)$$

For the special case of Poiseuille flow, the exponent  $b/2$  becomes equal to  $1/3$ , and recovers an old result of Murray [6] attempting to model the structure of the vascular system. This value was approximately applied to the prototype shown on Fig. 1. It is noteworthy that *the ratio of radii is independent of pore lengths, providing the pressure drop law (Eq. (8)) is the same at all scales*. If bifurcations were replaced by trifurcations, say, the factor 2 would just be replaced by a factor 3. Further scaling laws may be established for properties such as pore areas, pressure drop, dissipation and pore volumes. We just present the latter two.

4.2. Scaling laws for dissipation and pore volume

As an example of this approach, let us consider the scaling law of dissipation and pore volumes. Recall that the pore lengths are not in a constant ratio (see Eq. (4)); we must therefore distinguish two cases, according to the parity of  $k$ . The formulae in Table 1 are given as  $d_k$  for individual pores, and as  $D_k$  for the ensemble of the pores of class  $k$ . The scaling laws for total volumes of class  $k$  are obtained by combining Eqs. (4) and (21).

Examining the expressions for the relative overall dissipation (Eqs. (22) and (23)), it is seen that for  $b < 1$  (such as Poiseuille flow), the bifurcations which conserve the pore length ( $k$  odd, first column) result in an increase of dissipation ( $D_k$  is larger than  $D_{k+1}$ ), while the bifurcations where the pore length decreases always result in a decrease of dissipation (see the inequality signs). To get a more global and homogeneous result, it is appropriate to consider the dissipation ratio of two scales apart by two levels, that is  $D_k/D_{k+2}$ . This is done simply by multiplying Eqs. (22) and (23), after the appropriate change in index. We then obtain, irrespective of  $k$  being odd or even:

$$\frac{D_k}{D_{k+2}} = \frac{\text{dissipation at scale } k}{\text{dissipation at scale } k + 2} = 2^{b-1} \cdot 2^b = 2^{2b-1} \quad (27)$$

This quantity is larger than 1 for  $b > 1/2$  (such as the Poiseuille case), meaning that *dissipation globally decreases toward the smaller scales* (increase of  $k$ ).

Interesting corollaries are obtained for other quantities and summarized as follows:

The pressure drop ratios [ $\Delta p_k/\Delta p_{k+1}$  and  $\Delta p_k/\Delta p_{k+2}$ ] and the overall pore volume ratios [ $V_k/V_{k+1}$  and  $V_k/V_{k+2}$ ] obey exactly the same relationships as dissipation, that is, they scale as defined by Eq. (27). This can be seen for volume by comparing Eq. (24) to Eqs. (22), (23). This also means that *at any scale  $k$ , the dissipation, the pressure drop, and the total pore*

*volume are in a constant ratio*. On the other hand, the flow cross-section  $S_k$  and the wall surface area  $A_k$  of the pores, which is of interest when designing heat exchangers for example, scale in reverse, that is the exponents have the opposite signs.

4.3. Pore volume distributions

The volume fraction  $\varepsilon_k$  of each pore size in the optimal construct is defined as a function of the total number of scales  $m$  by:

$$\varepsilon_k = \frac{V_k}{V_p(m)} = \frac{V_k}{V_1} \frac{V_1}{V_p} \quad (28)$$

where the ratios  $V_k/V_1$  are given by Eq. (24), and  $V_p/V_1$  is calculated by:

$$\begin{aligned} \frac{V_p}{V_1} &= \sum_{k=1}^{k=m} \frac{V_k}{V_1} = \sum_{k=1}^m \frac{l_k}{L} \frac{L}{l_1} 2^{(1-b)(k-1)} \\ &= \sum_{k=1}^m \frac{l_k}{L} 2^{(1-b)(k-1)+2} = 2^{b+1} \sigma(m) \end{aligned} \quad (29)$$

The second equality of Eq. (29) is obtained by using the explicit formulae for the volumes and Eq. (17). The third equality is obtained by letting  $L/l_1 = 2^2$  and the fourth by factoring out the constructal function  $\sigma$ . Note that the quantity appearing in Eq. (29) (i.e.  $V_p/V_1$ ) was designated by  $\psi(m)$  in [4], and that there is thus a simple relation between  $\psi$  and  $\sigma$ . We found the latter function more general and analytically summable. The volume fractions  $\varepsilon_k$  are then obtained by combining Eqs. (25) and (29) (see Table 2).

The histogram of the volume fraction distribution is shown in Fig. 6 for  $m = 8$  and  $m = 20$ . Obviously, when the number

Table 1

Parity of $k$	$k = 1, 3, 5, \dots$	$k = 2, 4, 6, \dots$
Pore length	$l_k = l_{k+1}$	$l_{k+1} = l_k/2$
Pore flow rate	$f_{k+1} = f_k/2$	$f_{k+1} = f_k/2$
Pore radius	$r_{k+1} = r_k 2^{-b/2}$	$r_{k+1} = r_k 2^{-b/2}$
Dissipation $d_k$	$f_k \Delta p_k = \frac{a f_k^{q+1} l_k \mu}{\pi r_k^p}$	$f_k \Delta p_k = \frac{a f_k^{q+1} l_k \mu}{\pi r_k^p}$
Dissipation $d_{k+1}$	$d_{k+1} = d_k \cdot 2^{-b}$	$d_{k+1} = d_k \cdot 2^{-b-1}$
Relative overall dissipation $\frac{D_k}{D_{k+1}}$	$= \frac{d_k}{2d_{k+1}} = 2^{b-1}$	$= \frac{d_k}{2d_{k+1}} = 2^b = \left(\frac{r_k}{r_{k+1}}\right)^2 > 1$ (22), (23)
Relative pore volume	$\frac{V_k}{V_{k+1}} = 2^{b-1}$	$\frac{V_k}{V_{k+1}} = 2^b$ (24)
	$\frac{V_k}{V_1} = 2^{((1-2b)(k-1))/2}$	$\frac{V_k}{V_1} = 2^{((1-2b)k)/2+b-1}$ (25)
	$\frac{V_k}{V_1} (\text{Poiseuille}) = 2^{(1-k)/6}$	$\frac{V_k}{V_1} (\text{Poiseuille}) = 2^{(4-k)/6}$ (26)

Table 2

Parity of $k$	Odd: 1, 3, 5, 7, ...	Even: 2, 4, 6, 8, ...
Volume fraction of class $k$ , $\varepsilon_k$	$\sigma^{-1} \cdot 2^{(k(1-2b)-3)/2}$	$\sigma^{-1} \cdot 2^{(k(1-2b)-4)/2}$ (30)
Volume fraction $\varepsilon_k$ for Poiseuille flow	$\sigma^{-1} \cdot 2^{-k/6-3/2}$	$\sigma^{-1} \cdot 2^{-k/6-2}$ (31)



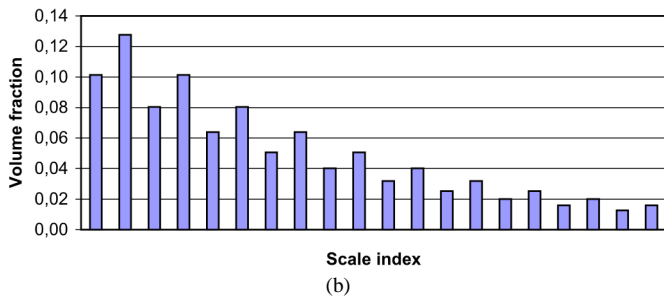
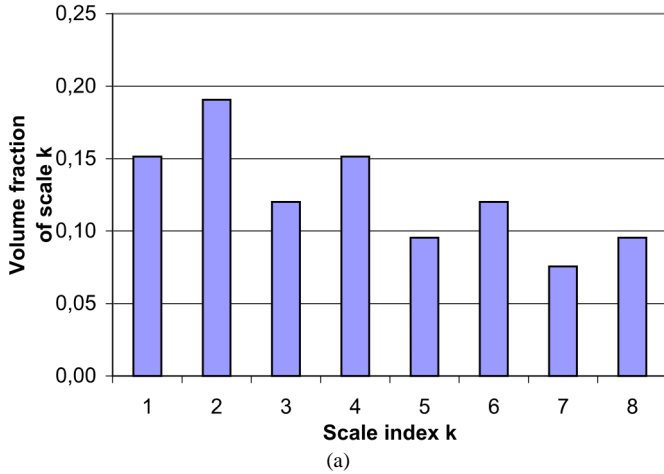


Fig. 6. Distribution of volume fractions for dichotomic construct ( $m = 8$  and  $m = 20$ ); this distribution holds as well for partial pressure drop and partial dissipation.

of scales  $m$  becomes larger, the contributions of each scale becomes smaller and smaller, and more so for the smallest scales. A further interesting relation may easily be obtained for the cumulative volume distribution, using Eq. (29):

$$\frac{\text{pore volume up to class } k}{\text{total pore volume}} = \frac{1}{V_p} \sum_{k=1}^k V_k = \frac{V_1}{V_p} \sum_{k=1}^k \frac{V_k}{V_1} = \frac{V_1}{V_p} 2^{b+1} \sigma(k) = \frac{\sigma(k)}{\sigma(m)} \quad (32)$$

Fig. 7 shows this distribution for  $m = 20$ . An essential point is that the histogram of Fig. 6 is identical for fractional dissipation  $D_k/D_{\text{tot}}$  and fractional pressure drop  $\Delta p_k/\Delta P_{\text{tot}}$ , and the histogram of Fig. 7 is identical for cumulative dissipation and cumulative pressure drop.

### 5. The case of equipartition of dissipation: the fractal dichotomic distributor

With the general theoretical background in hand, it is worth examining whether equipartition of the dissipation, or of entropy production, between the different scales makes sense, and leads to a situation of interest (see, for example [3,7] for discussions of this concept). For this purpose, we need to relax the constraint on the pore lengths, and let them become an optimization parameter, and impose equipartition of dissipation instead. We keep the “optimal” ratio of the radii (Eq. (21)) however. Expressing again the dissipation ratio  $D_k/D_{k+1}$  with

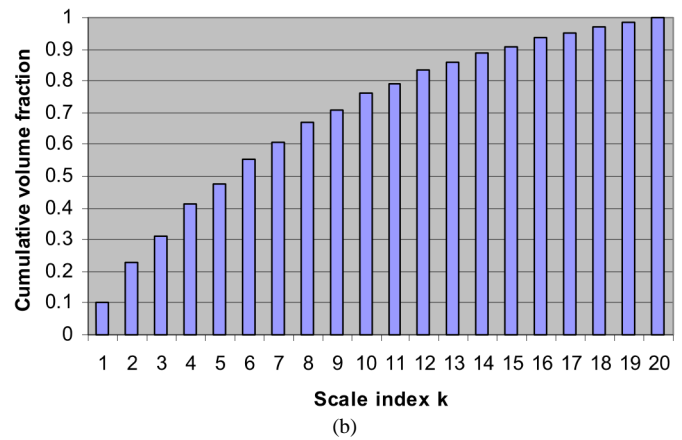
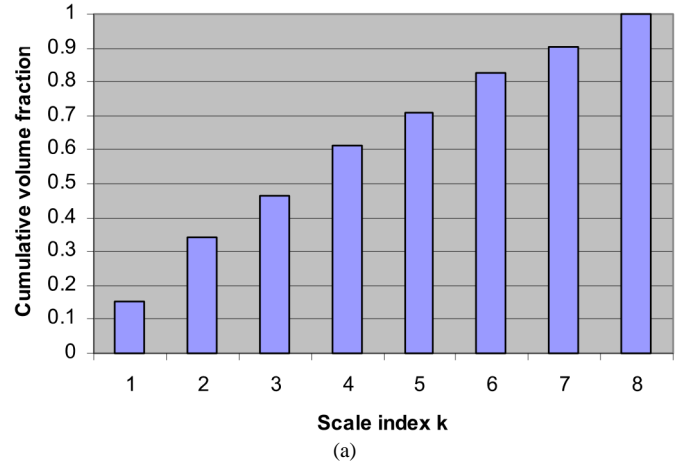


Fig. 7. Cumulative volume distributions for dichotomic construct ( $m = 8$  and  $m = 20$ ); this distribution holds as well for cumulative pressure drop and cumulative dissipation.

$f_{k+1} = f_k/2$  and  $r_{k+1} = r_k 2^{-1/3}$ , but letting  $l_{k+1}$  free, we obtain:

$$\frac{D_k}{D_{k+1}} = \frac{l_k}{l_{k+1}} \cdot 2^{-1/3} \quad (33)$$

Imposing that this ratio be equal to 1 for all  $k$  (equipartition of dissipation) yields:

$$\frac{l_k}{l_{k+1}} = \frac{r_k}{r_{k+1}} = 2^{1/3} \approx 1.26, \quad \frac{l_k}{l_1} = 2^{(1-k)/3} \quad (34)$$

Contrarily to the case studied above, the pore lengths change with every scale change, and are in the same ratio as their radii. The same result was obtained by Bejan [2] as a result of the minimization of flow resistance under the constraint of allocating a given area to a construct, which may be expressed as  $2l_k l_{k+1} = \text{constant}(k)$ . The meaning of this constraint is in principle one of “compactness”, or space saving, not of equidistribution. Area allocation on one hand, and equipartition of dissipation on the other hand, thus lead to the same scaling laws for both lengths and radii. We can therefore consider these approaches as equivalent, in this sense. The object that we thus define is a “pseudo-fractal”: the scaling rules are invariant with scale (there is no difference between even and odd generations).

What are the properties of this “equipartitioned” construct, compared to the previous one, recalling that the scaling law for

radii is the same? First, the path length from inlet to outlet is given by summation on Eq. (34), giving:

$$\sum_{k=1}^{k=8} l_k = l_1 \sum_{k=1}^{k=8} 2^{(1-k)/3} \approx 1.02L \quad (35)$$

This value is to be compared to the value of  $0.94L$  found above (Eq. (5)) for the “non-equipartitioned” structure (compare also the limits when  $m$  becomes large, approximately  $1.2L$ , as compared to  $L$ ). The path length in the equipartition case is therefore longer, in other words, this structure is in fact less compact! This property is actually verified from the fifth generation up. The fact of changing the scale rules between even and odd generations allows more compactness than a pure fractal with full scale invariance.

The equipartitioned case is therefore disadvantageous, not only with respect to compactness, but also with respect to hold-up dissipation and pressure drop. In addition, it cannot ensure uniform distribution over a pre-specified surface. From the point of view of distributor design, equipartition of dissipation and full scale invariance therefore yield poorer performances than the construct proposed here.

A further property of this structure is that the volumes  $V_k$  of all scales are identical (equipartition of pore volume over scales), as may be verified by calculating the ratio  $V_k/V_{k+1}$  using Eq. (34). Since dissipation is equipartitioned over scales by our premise, this implies that the theorem on equipartition (uniformity) of dissipation over volume (dissipation density) also holds.

## 6. Extension to different branching topologies

As an illustration, consider the construct of Fig. 8 which is under investigation in our team, and which also distributes a fluid onto a square surface through  $4^4 = 256$  regularly spaced outlet ports. The basic difference with the previous case is of course the quaternary division (quadrichotomy), with the consequences that the number of divisions, thus of scales, is divided by two to reach the same final resolution (here, 256), and the channel length is divided by two at each generation change. We thus have a regular pattern for the channel length, contrarily to the dichotomic case. The other difference is the existence of lateral connections (symbolized by squares) between division points of a given class. The purpose of these connections is to equilibrate the pressures between these points and therefore to compensate for possible geometric irregularities. In a “perfect” construct, there should be no flow in these connections. For the present purpose, we shall ignore them.

The constitutive relations are then:

$$\begin{aligned} n_k &= 4^k, & n_k/n_{k+1} &= 1/4, & l_k/l_{k+1} &= 2 \\ l_k/L &= 2^{-k-1/2}, & f_k/f_{k+1} &= 4, & f_k &= f_0/4^k \end{aligned} \quad (36)$$

The first branches have a length  $l_1$  equal to one quarter of the diagonal of length  $2^{1/2}L$ . The factor 2 of the previous case is replaced by 4 wherever it appears. The calculations may be carried out according to the same procedure. It is found for example that Eqs. (12), (13) and (21) are conserved provided the

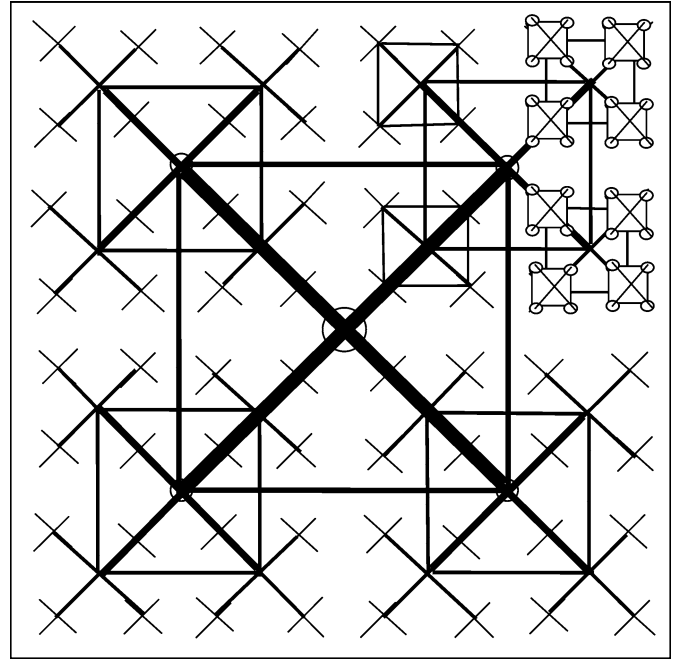


Fig. 8. Schematics of a quaternary-branched distributor; the lateral connections, materialized by squares, are not accounted for in the theoretical approach.

factor 2 is replaced by 4. Interestingly, the equations involving  $\sigma$  are conserved as well provided the definition of the constructal function is modified in the same way, replacing 2 by 4. We designate by  $\sigma_4$  this new constructal function, the subscript 4 referring to the quadrichotomy, and we have:

$$\begin{aligned} \sigma_4 &= \sum_{k=1}^m 4^{k(1-b)} \frac{l_k}{L} = \sum_{k=1}^m 4^{k(1-b)} \cdot 2^{-k-1/2} \\ &= \sum_{k=1}^m 2^{k(1-2b)-1/2} = \frac{1 - 2^{k(1-2b)}}{\sqrt{2}[2^{-(1-2b)} - 1]} \\ \sigma_4(\text{Poiseuille}) &= 2.72(1 - 2^{-m/3}) \end{aligned} \quad (37)$$

The last equality results from the summation of the geometric series with factor  $2^{1-2b}$ . There is no simple relation between  $\sigma_4$  and  $\sigma = \sigma_2$  introduced previously because the ratios  $l_k/L$  obey different rules. With this new  $\sigma_4$ , Eqs. (14) and (18) remain valid. The main scale relations for the different quantities are summarized below and it is of interest to compare the exponents to the dichotomic case.

$$\begin{aligned} \frac{r_k}{r_{k+1}} &= 4^{\frac{b}{2}} = 2^b, & \frac{d_k}{d_{k+1}} &= 2^{3-bp}, & \frac{D_k}{D_{k+1}} &= 2^{1-bp}, \\ \frac{\Delta P_k}{\Delta P_{k+1}} &= 2^{3-bp}, & \frac{V_k}{V_{k+1}} &= 2^{2b-1}, & \frac{V_k}{V_1} &= 2^{(1-k)(2b-1)} \\ \frac{V_k}{V_1}(\text{Poiseuille}) &= 2^{(1-k)/3}, & r_k^2 &= \frac{V_p}{\pi L} \frac{4^{-kb}}{\sigma_4} \\ \Delta P_{\text{tot}} &= 2A f_0^q (\pi L \sigma)^{p/2+1} V_p^{-p/2} \end{aligned} \quad (38)$$

Several features are noticeable: first, the pressure drop expression is identical to that of the dichotomic case; second, the volume does not scale as pressure drop or dissipation, but instead has the same exponent as  $V_k/V_{k+2}$  in the dichotomic case,



$2b - 1$ . Third, for Poiseuille flow, it turns out that  $2b - 1 = 3 - bp = 1/3$ , so that the exponents for volume, local dissipation and pressure drop are identical and express a decrease toward the smaller scales. An essential result is that *the theorem of uniform dissipation density is valid for this structure*. This may be verified by establishing that the ratio  $d_k/v_k$  (local dissipation density) is independent of  $k$ , using successively Eqs. (8) and (9) for the expression of  $d_k$ , Eq. (36) relating  $f_k$  and  $f_0$ , and Eq. (17) for the optimal pore radius. It is then found that the terms depending on  $k$  are in the exponents of 2 or 4 and finally cancel. As a result,  $d_k/v_k$  is also equal to the ratios  $D_k/V_k$  and  $D_{\text{tot}}/V_p$ , (obtained by summations of the numerator and denominator of  $d_k/v_k$ ), and this establishes the theorem.

Clearly, a similar approach can be transposed to other divisions as 2 or 4, such as trichotomy. The results imply a factor 3 instead of a factor 2 or 4, and a new  $\sigma_3$  function is introduced. The extension to combinations say of dichotomy and trichotomy, or any other combinations, is in principle straightforward, but the compactness of the results is lost.

## 7. Experimentation on distributors

Our research teams are carrying out experimental work on various constructal structures (distributors, mixers, heat exchangers). As a preliminary illustration, Fig. 9 visualizes the invasion of the dichotomic tree distributor (a “flat” version) by a fluid carrying an optical tracer (particles used in PIV experiments). The pictures are a small sample of that taken by a fast camera, and show the structure from above at different instants of time. The time span involved is a fraction of a second. These pictures clearly illustrate the inhomogeneity of the invasion: not all channels of a given scale are reached at the same time, and there will be a flow dispersion and a residence-time distribution, which may be quantified through these experiments, thus a departure from the ideal distribution (plug-flow type) assumed in all the theoretical developments above. This point will not be discussed further here but obviously calls for a theoretical approach that accounts for departure from plug-flow.

## 8. Discussion and conclusions

With respect to Ref. [4] addressing the same problematic of pore-size optimization under constraint of total pore volume, a number of new features are brought forward in the present article, while remaining in the framework of isothermal idealised plug-flow. First, the analytical approach introduced in [4] for the binary-branched tree has been extended with a more general flow equation, and fully explicit and compact solutions have been obtained for the various geometric and engineering quantities (pore radii distribution, volume fraction distribution, pressure drop, viscous dissipation) by formal summation of the series involved. In doing this, the notion of “constructal function”  $\sigma$  has been introduced, as a summable series depending only on the branching pattern and the flow equation, but independent of the other physical or geometric parameters. Quantities such as optimal pore radii, total pressure drop, volume fraction distribution may then be expressed in terms of this

function. Although odd and even classes of pores do not obey the same relations and display different dissipations, a general property emerges, stated as the theorem of *uniform dissipation density at all scales*.

The properties of this construct are compared to one in which the dissipation (not the dissipation density!) is postulated to be uniformly distributed, resulting in a fractal structure (all properties are scale invariant). The latter, besides not having a uniform irrigation of the outlet surface, is less compact and globally less performing.

A similar development has been carried out for a fractal-like quaternary-branched structure with uniform irrigation, for which the scale relations of pore length are simpler than for the binary branching (they do not depend on parity of the branch). All the previous analytical results are extended to this structure using a new constructal function specific of this topology. The theorem of uniform dissipation density is shown to apply here as well.

A qualitative visualization of the invasion of the structure by a tracer-flow is shown, which paves the way for further studies on flow non-idealities and their quantification.

Let us discuss a point which has been briefly addressed in the beginning of this paper, namely that of pressure-drop minimization instead of dissipation. It is found that if total pressure-drop is used to form the Lagrange function instead of total dissipation, and the optimization carried out in the same way, the same results are obtained: Eq. (14) for  $\sigma$ , Eq. (17) for  $r_k$ , Eq. (18) for total pressure drop, scale Eqs. (22)–(26). As a result, since the length distribution is the same, the relations for dissipation and the pore volume distribution are the same. Minimizing pressure drop or minimizing dissipation are therefore equivalent, illustrating the close physical connection between these notions.

The question that then arises is whether it is useful to introduce dissipation. We believe it is the case for two reasons. The first reason lies in the possibility to define a dissipation density and to state a general result such as the uniform dissipation density theorem, valid for all constructs discussed here. Recall that in the dichotomic construct, dissipation density is uniform whereas pressure drop is not equal in channels of different generations (that have different volumes). It would therefore not be possible to state a conservation or equipartition property in terms of pressure drop. The second reason is outside the scope of the present paper and concerns processes where phenomena other than viscous flow, such as heat and/or mass transfer, would contribute to dissipation. Dissipation, or even more generally, entropy production, is then a more appropriate notion for optimization.

A different line of thought around the same concepts is to consider the deterministic structure as a random porous medium and introduce the methods, models and variables pertinent to this domain. As a hint, suppose we wanted to characterize the structure by some kind of permeability or permeance, defined as the ratio of overall flow-rate ( $\text{m}^3 \cdot \text{s}^{-1}$ ) to the total pressure drop (Pa). Eqs. (18) or (19) obviously furnish such a relation. The ratio  $f_0/\Delta P$  does not furnish a conventional permeance, usually defined per unit cross-sectional area ( $\text{m} \cdot \text{s}^{-1} \cdot \text{Pa}^{-1}$ ), because the cross-sectional area of the construct is variable, and

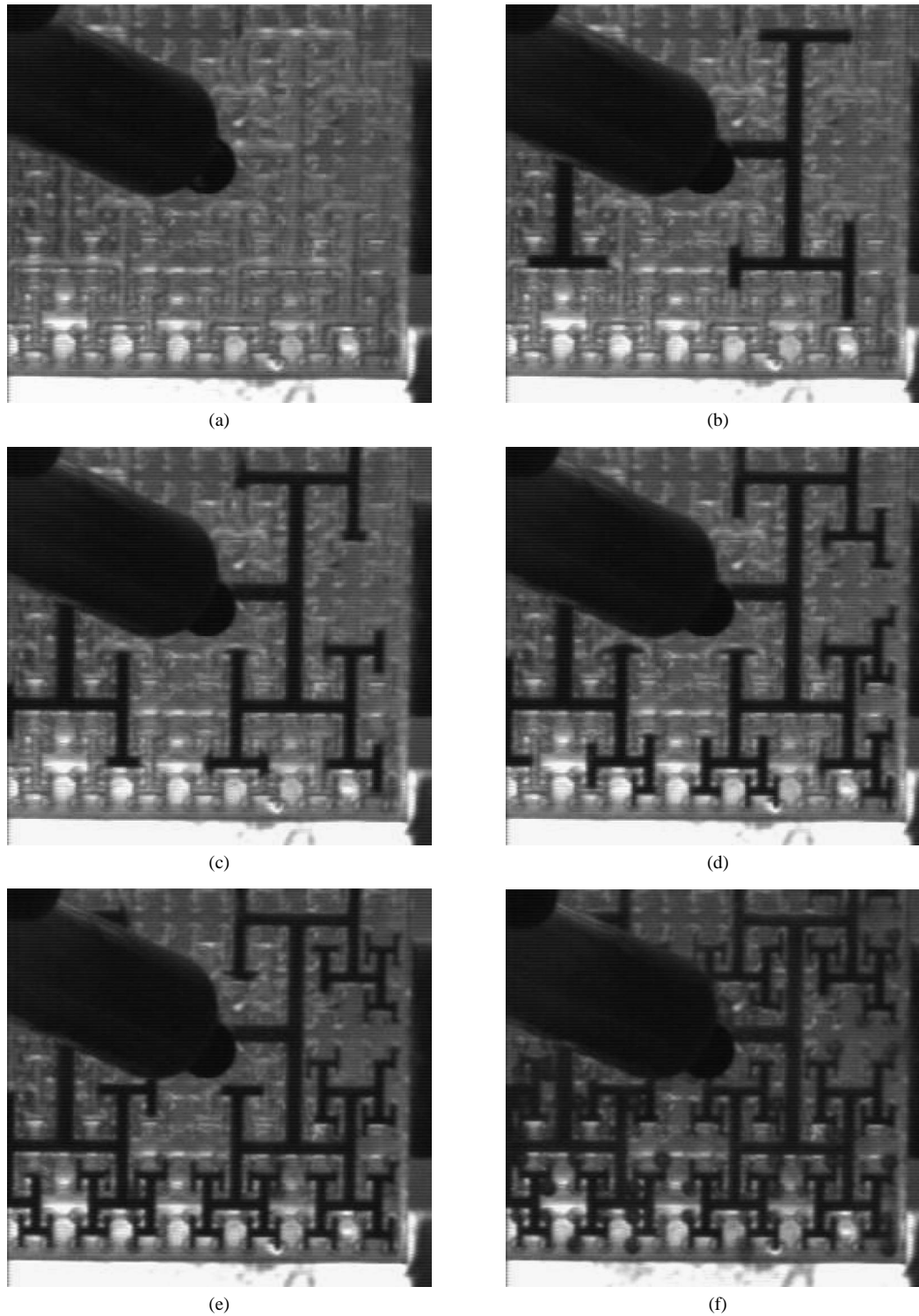


Fig. 9. Invasion of binary-branched structure by a tracer-liquid. Photographs are ordered at increasing times from left to right and top to bottom.

so is the flow velocity. A conventional permeance would therefore be a variable or would have to be averaged, thus limiting the interest of this notion.

Finally, we should like to address briefly the issue of *optimization of the number of scales*. In the present approach, this number is not an optimization variable but a decision variable chosen a priori by the designer on the basis of the “fineness”

of the irrigation (number of outlet ports per unit surface, say), or alternately, defined by the number of channels or tubes that need to be fed. Increasing the fineness of irrigation, thus the number of scales, implies increasing the total pore volume (see the numerical example in [4]). The latter is not an optimization variable, because just as the number of scales, it is maintained constant during the optimization.

Suppose now that there was a device downstream of the outlet ports, achieving a finer distribution on the whole surface, not just at discrete points, such as a fine grid or porous plug, having itself a flow resistance. The question is then how the overall resistance should be distributed between the branched distributor and this grid, and therefore how many branching scales are useful. If we assume that the pressure drop in the grid is proportional to the average distance of a point of the irrigated surface to an outlet port, then this quantity decreases when the fineness of the distributor thus the number of scales  $m$  increase (specifically, for the dichotomic case, this distance is divided by two at every increase of  $m$  by 2). On the other hand, the pressure drop in the branched distributor increases as  $\sigma(m)$ . The total pressure drop is thus the sum of a decreasing function and of an increasing function of  $m$ , leading obviously to some optimal number of scales. Formulated in this way, the problem is closer to that commonly addressed with the constructal approach, the problem of cooling a poorly conducting surface by distributing into it a good conducting material. In this case, as discussed recently in detail by Ghodoossi [8], the number of scales should be considered as an optimization variable. Depending on the respective resistances, this optimal may well correspond to a small number of scales, for which the general recurrent relations presented here are not needed.

## Acknowledgements

This work is supported by the French Agence de l'Environnement et de la Maîtrise de l'Energie.

## References

- [1] A. Bejan, *Advanced Engineering Thermodynamics*, Wiley, New York, 1997 (Chapter 13).
- [2] A. Bejan, *Shape and Structure, from Engineering to Nature*, Cambridge University Press, Cambridge, 2000.
- [3] A. Bejan, D. Tondeur, Equipartition, optimal allocation, and the constructal approach to predicting organization in nature, *Rev. Gén. Therm.* 37 (1998) 165–180.
- [4] D. Tondeur, L. Luo, Design and scaling laws of ramified fluid distributors by the constructal approach, *Chem. Engrg. Sci.* 59 (8–9) (2004) 1799–1813.
- [5] J.C. André, S. Corbel (Collective), *Stéréophotolithographie laser*, Polytechnica, Paris, ISBN 2-84054-021-5, 1994.
- [6] C.D. Murray, The physiological principle of minimum work, I. The vascular system and the cost of blood volume, *Proc. Nat. Acad. Sci.* 12 (1926) 207–214.
- [7] E. Kvaalen, D. Tondeur, Equipartition of entropy production: an optimality criterion for transfer and separation processes, *Ind. Engrg. Chem. Res.* 26 (1987) 50–56.
- [8] L. Ghodoossi, Conceptual study on constructal theory, *Energy Conv. Manag.* 45 (2004) 1379–1395.